RFTemp : Monitoring Microwave Oven Leakage to Estimate Food Temperature

AVISHEK BANERJEE, The Ohio State University, USA
KANNAN SRINIVASAN, The Ohio State University, USA

Microwave ovens have been widely used in recent years to heat food quickly and efficiently. Users estimate the time to heat the food by prior knowledge or by trial and error process. However, this often results in the food being over-heated or under-heated, destroying the nutrients. In this paper, we present **RFTemp**, a system that can monitor microwave oven leakage to estimate the temperature of the food that is being heated and thus estimate the accurate time when the food has reached the targeted temperature. To design such a system, we propose an innovative microwave leakage sensing procedure and a novel water-equivalent food model to estimate food temperature. To evaluate the real-world performance of RFTemp we build a prototype using software defined radios and conducted experiments on various food items using household microwave ovens. We show that RFTemp can estimate the temperature of the food with a mean error of $5°C$, 2x improvement over contactless infrared thermometer and sensors.

CCS Concepts: • **Computer systems organization → Sensor networks**; • **Human-centered computing → Ubiquitous and mobile computing design and evaluation methods**.

Additional Key Words and Phrases: Microwave Oven, Radio Frequency Sensing, Dielectric Heating, Food Temperature Estimation, Dielectric Property, Real-time

ACM Reference Format:
Avishek Banerjee and Kannan Srinivasan. 2021. RFTemp : Monitoring Microwave Oven Leakage to Estimate Food Temperature. *Proc. ACM Interact. Mob. Wearable Ubiquitous Technol.* 5, 4, Article 144 (December 2021), 25 pages. https://doi.org/10.1145/3494967

1 INTRODUCTION

Over the past few years, advancement in intelligent wireless sensing technologies has improved human interaction with various household devices and appliances. With the development of various smart sensing applications like vibration sensing [46, 52], pressure sensing [21], electrical sensing [23, 37, 38], audio sensing [16], temperature sensing [13], camera-based sensing [19, 20] has allowed us to monitor and control various indoor appliances to a great extent. However, all such techniques require installation of specific hardware sensors for respective applications which becomes costly and requires high maintenance.

On the other side, Radio-Frequency (RF) sensing has also been widely used in recent works to leverage information from the RF environment. Various RF sensing techniques like WiFi, RF identification (RFID), acoustics, ultra-wideband (UWB) have been widely used to localize and monitor human activities [34, 42, 49] to control various indoor smart devices [29, 43, 48]. Even though RF sensing provides a low-cost and ubiquitous

Authors' addresses: Avishek Banerjee, The Ohio State University, Computer Science and Engineering, Ohio, USA, banerjee.152@osu.edu; Kannan Srinivasan, The Ohio State University, Computer Science and Engineering, Ohio, USA, kannan@cse.ohio-state.edu.

2474-9567/2021/12-ART144 $15.00
https://doi.org/10.1145/3494967

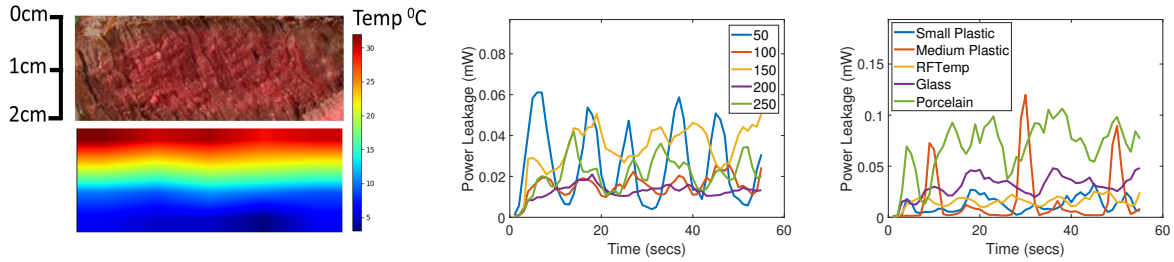

(a) (b) (c)

Fig. 1. (a) Variation of temperature at different thickness levels (0-2cm) for a steak heated for 1 minute. The average temperature of the food measured after heating is around $15^{\circ}C$. Infra-Red (IR) thermometer measured $30^{\circ}C$ ($\sim 15^{\circ}C$ error), RFTemp estimated the final temperature $18^{\circ}C$ ($\sim 3^{\circ}C$ error). (b) Leakage observed by heating 50-250 gm of water for 1 minute in a plastic container. (c) Leakage observed by heating 100 gm of water for 1 minute in different containers. RFTemp container is the container used to develop our water model described in Sec. 5. The leakage pattern varies across different weights and containers.

service compared to hardware sensors, it cannot be directly used for physical measurements like humidity and temperature.

Microwave oven, also referred to as microwave, is one of the most commonly used appliances in household and commercial kitchens. Recent research suggested that around 13 million microwave ovens have been shipped in the United States during the year 2019 [8] and around 96% of the households use microwave oven [51]. Microwave ovens heat and cook food using dielectric heating by exposing food to high-frequency electromagnetic radiation which is absorbed by polar molecules (like water) in food. Most modern microwave ovens require users to manually set the cooking or heating time for a particular food. The required time to cook food to a targeted temperature in a microwave oven depends on factors like the orientation of the food, microwave container surface area, dimensions and power output of the microwave oven. It also depends on initial temperature of the food, moisture content, thermal conductivity, and thickness of the food. However, this process requires complex calculations, and it is not feasible for any user to estimate the correct time to heat or cook the food without knowing the above-mentioned factors accurately. Users either estimate the time to heat food by prior knowledge of trial and error technique or keep on checking the temperature of the food and repeat the process until the target temperature has reached. This process is highly time-consuming and often results in overheating of the food, destroying nutrients. Research survey [51] shows around 75% of users use the microwave oven more than thrice a day. Thus, such error in estimation can have a negative impact on human health in a long run.

However, we notice that the above challenge to measure the temperature of the food in the microwave oven has been researched extensively. Camera-based techniques [5, 6, 15, 17, 31], installation of Infra-Red (IR) temperature sensors [14, 30, 33, 44], image classification and temperature sensing technique [26, 31], monitoring leakage to classify food types [50] have successfully addressed the problem to great extent. However, these techniques mostly need direct contact with the food or require installation of sensors and cameras on the microwave oven which is not cost-efficient and cannot be installed by users easily. Over that, temperature sensors and thermal cameras can only measure the temperature of the surface of the food [41]. Fig. 1(a) shows the thermal map after heating steak for 1 minute. As we can see, with increasing thickness, the temperature decreases from the surface. Thus, for thick food like meat, the infrared sensors and cameras can result in errors in temperature estimation of the food as the surface heats faster than inside. Even the machine learning and image processing-based approach can only successfully classify a given set of food of a particular weight and using a specific container. Fig. 1(b) shows the leakage observed for different weights of water using a particular microwave container. Fig 1(c) shows

the leakage observed for 100 gm of water across different containers. As we can see from the figures, the leakages are quite different across weights and containers. This can severely affect the accuracy of the leakage classification techniques [50] if not taken under consideration and training models for all such weights, containers, and food combinations is not realistic.

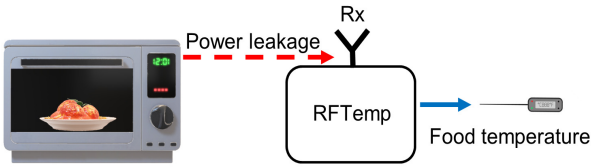

Fig. 2. Overview of RFTemp sensing microwave power leakage to estimate food temperature.

To address these challenges, in this paper, we present RFTemp, as shown in Fig. 2, an RF sensing system that can monitor leakage coming out from the microwave oven window to estimate the temperature of the food that is getting heated. Overall, the paper makes the following contributions:

1) We propose an intelligent RF sensing technique that can retrieve information from the microwave leakage and directly maps it to the amount of heat absorbed by the food.

2) We propose a novel water-equivalent food model that maps the food properties to an equivalent, known water model to determine the temperature and the properties of the heated food.

3) We propose a practical error correction technique that makes RFTemp robust to any microwave containers and distance of measurements.

To the best of our knowledge, we are the first to realize a practical contact-less RF sensing system to measure the temperature of the food being heated in a microwave oven without any extra hardware installation and can be integrated easily into existing systems. Table 1 shows the comparison between RFTemp and other state-of-the-art works.

Table 1. Comparison with other works

Work	Contactless temperature sensing	Hardware installation	Robust to containers and ovens	Robust to food with different thickness and types	Real time temperature sensing
E. Belotserkovsky et al. [14] (IR fiberoptic radiometer)	Yes	Yes	Yes	No	Yes
G. Cuccurullo et al. [17] (FLIR camera)	Yes	Yes	No	No	Yes
June Intelligent Oven [6] (RTD sensor)	No	Yes	Yes	Yes	Yes
T.Khan [26–28] (IR temperature sensors)	Yes	Yes	No	No	Yes
W. Wei et al. [50] (Microwave leakage and Machine Learning)	No	No	No	No	No
RFTemp (Fig. 2) (Microwave leakage sensing) (Proposed)	Yes	No	Yes	Yes	Yes

2 RELATED WORK

2.1 Thermal Imaging Based Techniques

Thermal imaging-based techniques have been well researched in recent years to estimate the temperature of the food in the microwave oven in real-time. Works like [15, 28] uses Forward-Looking InfraRed (FLIR) camera-based techniques to produce thermal imaging of the microwaved food. In [17], thermaCAM flir P65 camera was used to perform contactless thermal imaging of the food surface. [6] uses High-Definition (HD) camera to predict the cooking time of some predefined food items. All these works require the installation of cameras and sensors in the microwave ovens which is not cost-efficient and cannot be implemented easily on commercial microwave ovens. Low-cost thermal imaging techniques like temperature sensing using a Charge-Coupled Device (CCD) camera is proposed in [31] to sense the temperature inside the microwave oven. However, such techniques may not have high accuracy.

2.2 Temperature Sensor Based Techniques

Various temperature sensing techniques are used in recent works to measure the temperature of the food inside the microwave oven in real-time. However commercial low-cost temperature sensors can be highly affected by the electromagnetic radiations inside the microwave oven and cannot be used. Fiber optic sensors have been commonly used in such settings as they are not affected by such radiations [45]. However, such sensors require direct contact with the food, which is not hygienic and require cleaning before using every time. For contact-less sensing, [14] proposed an Infra-Red (IR) fibroptic temperature sensor to measure the temperature of the food. However, such techniques require the sensors to be placed very close to the sample and require extensive calibration. Works like [30, 33, 44] use feedback and control techniques using infrared sensors, cameras, and network analyzers to optimize the microwave heating. Such techniques cannot be implemented in commercial microwave ovens easily. Resistance temperature detector (RTD) sensor probes are used in [6], but such techniques require physical contact of the sensor probe to the food. Works like [26] used IR temperature sensor, [27] used 8X8 IR temperature sensors grid to measure the temperature of the food inside microwave oven. The sensors are placed on the oven roof with a 4mm hole inside the cavity to receive the IR signals. The electromagnetic radiations (wavelength $\sim$ 120 mm) cannot pass through the 4mm hole thus cannot affect the sensors. These sensors measure the surface temperature of the food only and will result in wrong estimations in thicker foods like meat.

2.3 Image Classification Techniques

Recent works also used image classification models to identify different food items and recommend temperature based on previous knowledge. In [26], an HD camera is used to take food pictures, and a histogram-based classification technique is used to identify the food. However, such techniques are highly dependent on the microwave-container color and the food color, which makes it difficult to implement on everyday food items. Convolution Neural Network (CNN) model is used in [28] to classify food images and recommend heating temperature based on previous knowledge. But this technique is also prone to erroneous classification for different container colors and shapes. A median filter approach is proposed in [31] to classify thermal images using a low-cost CCD camera. However, such techniques are not accurate on complex food items. [6] use an HD camera for capturing high definition images but can only classify a few predefined foods.

2.4 Microwave Leakage Classification

Microwave oven leakage has been used in recent work to classify different food items that are being heated [50]. However, such classification is not robust to different weights of food, container shape and size and can

only classify few predefined tested food. Training models for various such combinations is not realistic and time consuming.

3 MOTIVATION

Typical household microwave ovens operate at a frequency of 2.45 GHz with a bandwidth of only a few MHz [47]. They use a high-powered vacuum tube called magnetron [10] that converts the electrical input of the oven into a microwave signal that oscillates at 2.45 GHz. A wave-guide directs these signals from the magnetron into the metal cooking chamber of the microwave oven where it creates an alternating electromagnetic field [47]. In a microwave oven, the electrically bipolar molecules present in the food (like water) absorb most of these microwaves by a process called dielectric heating [11] and causes molecular vibration, which eventually results in heating the food. The important components of microwave heating are as follows:

3.1 Power Absorbed by Dielectric Material

The average power absorbed ($P_{abs}\ Watts/m^3$) by a dielectric of volume V is given by Eq. 1 [18], where ω is the angular frequency of microwave, $\epsilon_0 = 8.8542 * 10^{-12} F/m$ is the permittivity of free space, $\epsilon^{''}_{eff}$ is the effective loss factor of the dielectric and E is the microwave electric field.

$$P_{abs} = \omega \epsilon_0 \epsilon^{''}_{eff} E^2 V \tag{1}$$

To be noted that P_{abs} is the prime source of microwave heating that dissipates in the food.

3.2 Permittivity

The interaction of the dielectric with the electric field is characterized by its permittivity (ϵ). The permittivity of a dielectric is expressed by Eq. 2 [18], where ϵ_0 is the permittivity of free space and ϵ_r is the relative permittivity of the material. The ϵ_r is a complex term and can be expressed by a real part ($\epsilon^{'}$) also known as dielectric constant and an imaginary part ($\epsilon^{''}_{eff}$) as shown in Eq. 3.

$$\epsilon = \epsilon_0 \epsilon_r \tag{2}$$

$$\epsilon_r = \epsilon^{'} - j\epsilon^{''}_{eff} \tag{3}$$

$\epsilon^{''}_{eff}$ measures the losses when electromagnetic radiations are absorbed by the dielectric and $\epsilon^{'}$ determines lossless storage and how much radiation is reflected at the surface of the dielectric. Permittivity is an important measure of the property of the food. However, permittivity is temperature dependent and in most of the foods it decreases with increase in temperature [18].

3.3 Penetration Depth

Power penetration depth or simply the penetration depth δ_p of dielectric material is the measure of how far the electromagnetic fields can penetrate the material before it gets attenuated to one-third of its value on the surface [18]. Thus, food with a thickness smaller than δ_p absorbs the radiation uniformly compared to a thick food. The penetration depth can be expressed by Eq. 4 [3, 18], where λ is the wavelength of microwave signal and $\epsilon^{'} >> \epsilon^{''}_{eff}$ which is valid for most of the food materials. With increase in temperature δ_p decreases as $\epsilon^{'}$ decreases.

$$\delta_p = (\lambda/2\pi)(\sqrt{\epsilon^{'}}/\epsilon^{''}_{eff}) \tag{4}$$

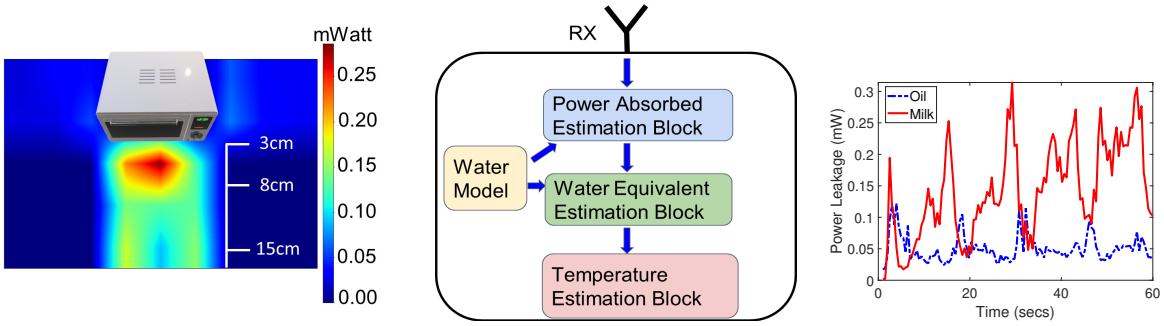

(a) (b) (c)

Fig. 3. (a) RF leakage around microwave oven. Maximum leakage occurs around 6 cm from the front door panel. (b) Simplified block diagram of RFTemp. (c) Typical microwave leakage observed for 60 secs for oil and milk.

3.4 Reflection Coefficient

When the microwaves hit the dielectric material, a part of it gets reflected, and a part penetrates the material. Permittivity is directly proportional to the square of the refractive index [47]. Thus using Eq. 4, we can say, penetration depth is inversely proportional to the square the complex part of the refractive index of the medium [47]. On the other hand, theoretical power-reflectance or the reflection coefficient is directly proportional to the refractive index of the material [18]. Thus, δ_p is indirectly related to reflection coefficient. Shallower the penetration depth, more is the reflection. Thus, with an increase in temperature, as penetration depth decreases, the reflection coefficient increases.

All these parameters play an important role in determining the temperature of the food getting heated in the microwave oven. However, to measure these properties explicitly, we require specialized instruments and direct access to the microwave oven food chamber. These can be highly dangerous as microwave radiation inside the food chamber is hazardous to human health and can cause damage to other electrical instruments [18]. Moreover, the food chamber acts as a Faraday cage that attenuates most of the electromagnetic radiation escaping from the oven [4]. United States Federal standard limits the amount of microwaves that can leak from an oven throughout its lifetime to 5 milliwatts (mW) of microwave radiation per square centimeter at approximately 2 inches from the oven surface. Thus a very small portion of the RF waves is able to penetrate through the microwave oven walls which makes the RF sensing highly difficult.

RFTemp addresses this challenge by proposing an intelligent sensing technique to retrieve useful information from the microwave leakage. Details of the process are described in Section 5.

4 OVERVIEW

Fig. 3(a) shows a heat map of the microwave leakage power around the microwave oven. As we can see, the maximum leakage occurs through the front-door panel of the microwave oven and, it gets attenuated with increasing distance. Even though microwave oven (operating at 2.45 GHz) shares the same RF spectrum as other household applications like WiFi, Bluetooth, however, the power density of these applications are several times smaller than the measured microwave leakage and thus causes no interference. RFTemp leverages this leakage in real-time to estimate the temperature of the food in the microwave oven. Fig. 3(b) shows the overall system design of RFTemp. Fig. 3(c) shows a typical leakage pattern observed by RFTemp while heating 100 gm of milk and oil respectively in the microwave oven for a duration of 1 minute. As we can see from the figure, the power leakage value varies in intervals of ~ 15 secs which is equivalent to one cycle duration of the turntable plate in the microwave oven [50]. Moreover, the leakage is different for oil and milk. We use this time varied power

leakage pattern to evaluate the food property and estimate the temperature of the food in the microwave oven. Details are described in Sec. 5.

5 DESIGN

In this section, we discuss the details of RFTemp.

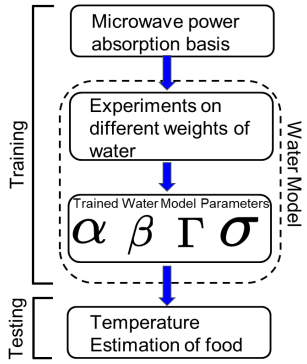

Fig. 4. Design overview

Fig. 4 shows the different stages of RFTemp design model. The first stage uses fundamental concepts of electromagnetic radiation to develop a simplified measurable power absorption variable. To estimate the power absorption and to find a relation with the microwave oven leakage, RFTemp introduces a novel water model. Based on the microwave absorption basis and experiments on water with different weights, the water model defines four different experimental parameters. Using these trained parameters, our system maps the leakage observed to the power absorbed by the food inside the microwave oven and develops experimental properties of water. These together make the training phase of our design model. The last part of our design model uses these trained water model parameters and the real time microwave oven leakage to estimate the temperature of the food. Each of these blocks are discussed in detail in this section.

5.1 Microwave Power Absorption Basis

As we have seen in Eq. 1, the power absorbed by any food in a microwave oven depends on the electric field strength E inside the oven. It is difficult to directly estimate this electric field strength as we have no access to the food chamber. RFTemp utilizes the fundamental concepts of electromagnetic radiation to solve this challenge. We develop a simple model assuming the electromagnetic radiation in microwave oven as plane waves in free space. Later in Sec. 5.2 we fit this simple model's parameter using experimental measurements.

As we know, the energy associated with the electromagnetic wave is the sum of the energies of the electric and magnetic fields as shown in Eq. 5, where u is the energy per unit volume or total energy density and u_e and u_b are the energy density of electric field and magnetic field respectively.

$$u = u_e + u_b \tag{5}$$

We can rewrite Eq. 5 based on [32, 36] as

$$u = \frac{1}{2}\epsilon_0 E^2 + \frac{1}{2\mu_0}B^2 \tag{6}$$

Since $E = cB = \frac{1}{\sqrt{\epsilon_0 \mu_0}} B$, where c is the speed of light,

$$u = \epsilon_0 E^2 \tag{7}$$

where E and B are the electric and magnetic field strengths respectively, ϵ_0 is the permittivity of free space and μ_0 is the permeability of free space. Thus, the energy flux (S) associated with the wave can be represented as

$$S = uc = \epsilon_0 c E^2 \tag{8}$$

The power per unit area (A) is the time average of this energy flux (S). Thus from Eq. 8 we can write,

$$\frac{P}{A} = \frac{1}{2} \epsilon_0 c E^2 \tag{9}$$

Thus, for a microwave oven with an average surface area of A_{avg} and output power of P_{micro} (~1000 Watt), we can write Eq. 9 as

$$P_{micro} = \frac{1}{2} \epsilon_0 c E^2 A_{avg} \tag{10}$$

Based on the above derivation we can rewrite Eq. 1 as

$$P_{abs} = \frac{4\pi}{\lambda} \epsilon''_{eff} \frac{V_{food}}{A_{avg}} P_{micro} \tag{11}$$

where, $\omega = \frac{2\pi c}{\lambda}$, λ is the wavelength of electromagnetic radiation. P_{abs} now depends on measurable variables and can be estimated. However, it is to be noted that V_{food} here is the volume of the food exposed to microwave radiation uniformly, that is, the thickness of the food is less than the penetration depth of the microwave signals.

5.2 Water Model

Even though Eq. 11 helps us to estimate the power absorbed by the food inside a microwave oven, it is difficult to explicitly measure both V_{food} and ϵ''_{eff}. This is because different types of food have different penetration depths due to their complex permittivity. Similarly, the ϵ''_{eff} term is dependent on the constituents of food like protein, fat, carbohydrate, and water. Thus estimating these factors for everyday food is not trivial. Moreover, it is not clear how the leakage observed through the microwave door is related to the power absorbed by the food. To address these challenges, we propose a water model to estimate the P_{abs} directly from the microwave leakage observed over time.

We conducted series of experiments with the weight of water ranging from 50-500 gm (at room temperature). We placed the receiver antenna (Rx) of the RFTemp at a 6 cm distance from the center of the microwave oven front door to measure the power leakage pattern $r(t)$ for each load of water microwaved for 15 secs duration. We physically measured the initial and final temperature of the water with a food thermometer. Most of the recent microwave oven has a turntable cycle of 15 secs. So the training interval for RFTemp was chosen to be 15 secs. However, this can be further reduced to a time less than 15 secs. Based on these experiments we defined the following terms.

5.2.1 Power Amplification Factor (α). From Eq. 11 we know $P_{abs} <= P_{micro}$. Most of this radiation that is not absorbed by the food ($E_{leakage}$) escapes through the front panel of the microwave oven after getting attenuated.

$$E_{leakage} = (P_{micro} - P_{abs}) \times \tau = E_{micro} - E_{abs} \tag{12}$$

where τ is the time duration in seconds and $E_{leakage}$ is the total leakage energy observed, and E_{abs} is the total energy absorbed for τ secs. Fig. 5(a) shows a typical power leakage pattern, $r(t)$, observed for $\tau = 60$ secs. Thus we can write,

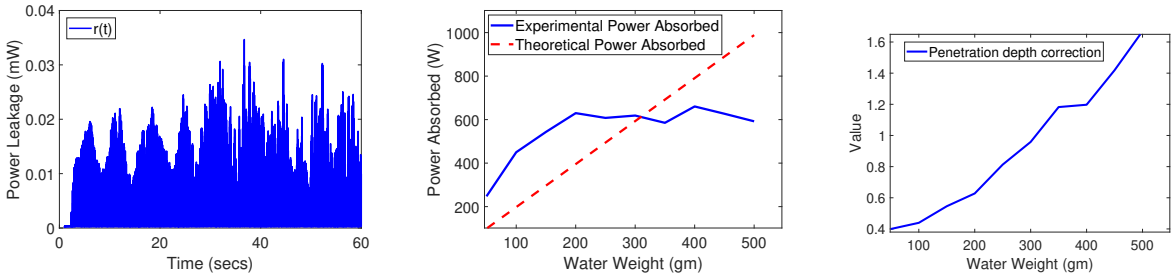

(a) (b) (c)

Fig. 5. (a) Power leakage observed by RFTemp for 1 minute by heating 100 gm of water in microwave oven. (b) Experimental and Theoretical power absorbed per second for different weights of water. (c) Penetration depth correction for different weights of water.

$$E_{leakage} = \alpha \sum_{t=0}^{\tau} r(t) \tag{13}$$

The power amplification factor (α) maps this leakage observed outside, $r(t)$, to the original power leakage inside the microwave oven. However, to estimate α we need to calculate E_{abs} based on Eq. 12 and 13.

Thus using the experimentally measured initial and final temperatures of different weights of water and the heat capacity relationship (Eq. 14) we calculated the heat energy absorbed by the equivalent mass of water for 15 secs duration.

$$E_{heat}(m,T) = P_{heat}(m,T) \times \tau = ms(t2 - t1) \tag{14}$$

where m and s are the mass and specific heat of water, $t2$ and $t1$ are the final and initial temperatures and $\tau = 15$ secs. E_{heat} is dependent on mass and temperature difference of the water. The blue line in Fig. 5(b) shows the power absorbed per sec by corresponding mass of water. Now E_{heat} is nothing but E_{abs} for the whole volume of water. Thus we can express α as

$$\alpha = \frac{(P_{micro} - P_{heat}(m,T)) \times \tau}{\sum_{t=0}^{\tau} r(t)} = \frac{E_{micro} - E_{heat}(m,T)}{\sum_{t=0}^{\tau} r(t)} \tag{15}$$

In the above mentioned experimental setup, for $\tau = 15$ secs, $\alpha \sim 150$ for all the experiments. Thus it is to be noted, the power amplification factor depends on experimental variables only like the distance between the receiver and microwave oven front panel, microwave oven output power, and the microwave container shape. It is independent of the properties of food. To address these experimental factors, we propose error correction techniques in Section 5.4.

5.2.2 Penetration Depth Correction ($\beta(m,T)$) . The red dotted line in Fig. 5(b)[1] shows the theoretical power absorbed P_{abs} for the same mass of water used for the power amplification factor calculations. P_{abs} is calculated using Eq 11, where $\epsilon''_{eff} \sim 10$ for water (at room temperature). As we can see from Fig. 5(b), P_{heat} experimental is highly uncorrelated with P_{abs} theoretical. The main reason behind this is, as the weight of water increases, the microwave radiation is not uniformly absorbed. To compensate for this error, we define the penetration depth correction factor β as the ratio between E_{abs} and E_{heat}, so that both the theoretical and experimental energy absorbed values map to the same mass of the food.

[1]In Fig. 5(b), to represent the power in watts we presented the time averaged values.

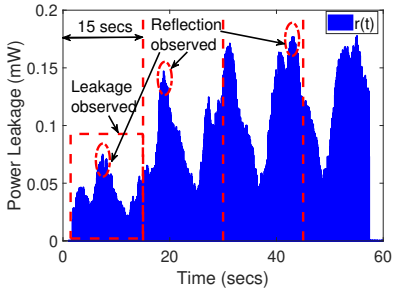

(a) Area under curve maps to the RFTemp dielectric coefficient and the max leakage maps to the reflection coefficient.

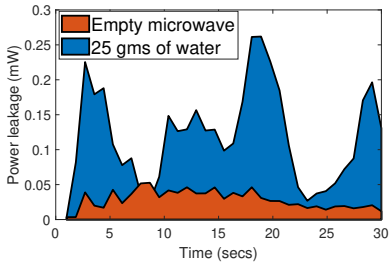

(b) Leakage observed with and without water.

Fig. 6. Leakage pattern observed by RFTemp

$$\beta(m,T) = \frac{E_{abs}(m,T)}{E_{heat}(m,T)} = \frac{P_{abs}(m,T) \times \tau}{P_{heat}(m,T) \times \tau} = \frac{P_{abs}(m,T)}{P_{heat}(m,T)} \tag{16}$$

Fig. 5(c) shows the $\beta(m,T)$ variation with different weights of water. It is to be noted that, this factor depends on the mass (m) and temperature (T) of the food. With increase in temperature P_{abs} decreases as ϵ''_{eff} decreases, thus β [2] decreases. However, during the training phase for 15 secs, β is independent of the temperature factor. It is only effective while measuring microwave leakage at the end of every 15 secs time slot as explained in the feedback block in Sec 5.3. β is calculated as the ratio between a theoretical quantity and an experimentally measured quantity. Both of them are independent of the experimental environment so β is also independent of experimental environment.

5.2.3 Reflection Coefficient ($\Gamma(m,T)$) . This experimental coefficient has an indirect relationship with the penetration depth of the food. Shallower penetration depth results in more reflection of the incident radiation. To address this factor, we introduce Γ [2], which is measured as the maximum leakage during one cycle of rotation of the microwave oven turntable ($\sim$ 15 secs). Fig. 6(a) shows a typical leakage pattern observed. It is a realistic estimation, as the leakage observed is directly proportional to the reflection of the incident wave on the food. To verify this claim, we experimented on 25 gm of water and an empty microwave.

As shown in Fig. 6(b), when there is no food in the oven there is a nominal leakage. However, in such a situation the leakage will slowly decrease with time. However, even there is a very small load like 25 gm of water, the leakage is quite dominant, and we can observe the cyclic pattern which is mainly because of the food present inside. Thus the leakage observed is related to the reflection of the microwave from the food items to certain extent. This reflection coefficient corrects for overestimation of the water equivalent of any food, explained in Sec. 5.3.

$$\Gamma(m,T) = max(r(n) : n = [0 \cdots 15]) \tag{17}$$

where n is measured in seconds and r is the leakage observed. As shown in Fig. 6(a), Γ is marked by the red dotted circles which is the maximum leakage observed in 15 secs interval. Γ is dependent on the mass and temperature of the food as the leakage pattern is different for different weights of water and with increase in temperature, reflection coefficient increases as mentioned in previous section. Similar to the penetration depth correction parameter, Γ varies with temperature after every 15 secs time slot.

[2] $\beta(m,T)$, $\Gamma(m,T)$ and $\sigma(m)$ are represented in many places as β, Γ and σ respectively for simplicity.

5.2.4 RFTemp Dielectric Coefficient ($\sigma(m)$). This parameter is used to measure the experimental dielectric property of water. It is expressed as the area under the power leakage curve $r(t)$. It is an experimental measure of the food property and how good they can absorb the radiation. We calculated σ [2] for different water experiments as the leakage pattern is different. We used these as training set. Thus it is dependent on the mass of water. Later in Sec. 5.3, we verified the accuracy of this parameter.

$$\sigma(m) = \sum_{t=0}^{\tau} r(t) \tag{18}$$

In Fig. 6(a), the area under curve marked by the red dotted box shows the leakage observed will heating 400 gm of water for 15 secs. It is to be noted that σ is an experimental parameter focused for your system.

The parameters β, Γ and σ are measured for weights of water within a range of 50 to 500 gm.

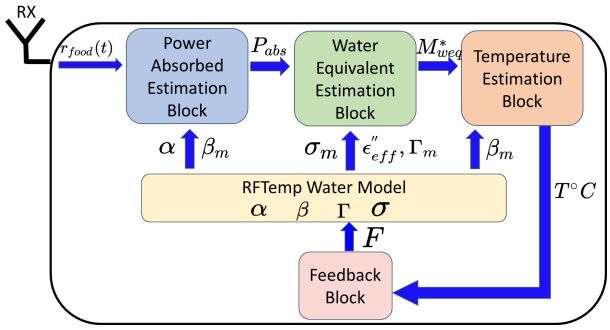

Fig. 7. Detailed block diagram of RFTemp. This flow is repeated every 15 secs.

This phase of defining the water model is called the RFTemp training phase. Using this trained water model as reference, our system estimates the temperature of the food every 15 secs that is being heated.

5.3 Temperature Estimation of Microwaved Food

Based on the proposed water model, RFTemp introduces the following design blocks to estimate the food temperature every 15 secs interval. Fig. 7 shows the complete workflow of RFTemp.

5.3.1 Power Absorbed Estimation Block . RFTemp observes the power leakage when the food is being heated and calculates $\sum_{t=0}^{\tau} r_{food}(t)$, where τ is equal to 15 secs duration. Now, with the known α, and corresponding β, calculated using the water model, we can estimate the power absorbed by the food inside the microwave oven by Eq. 19 and 20.

$$\alpha \sum_{t=0}^{\tau} r_{food}(t) = E_{leakage} \tag{19}$$

$$E_{abs} = \beta_m \times E_{heat} = \beta_m \times (E_{micro} - E_{leakage}) \tag{20}$$

where, β_m is the penetration depth correction factor for the particular mass of food (m) and $\sum_{t=0}^{\tau} r_{food}(t)$ is the area under the leakage curve. It is to be noted that β_m is taken from the water model parameter $\beta(m, T)$ which consists of series of values for different weights of water. For example, β_{100} represents the penetration depth correction factor value β for 100 gm of water.

5.3.2 Water Equivalent Estimation Block . From the calculated E_{abs} we can estimate the equivalent mass of water (M_{weq}) using Eq. 11. M_{weq} is the equivalent mass of water when replaced with the food, will absorb the same amount of radiation. The density of water is taken as 1 gm/cc.

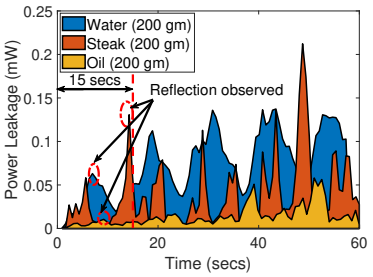

Fig. 8. Dielectric correction and reflection correction estimation of steak and oil.

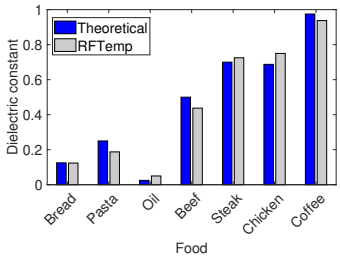

Fig. 9. Dielectric property of food with respect to water. RFTemp relative leakage values closely follow the dielectric property of the food.

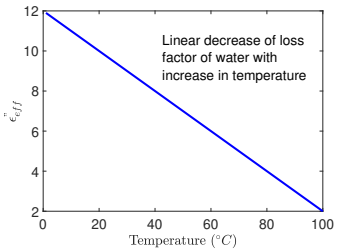

Fig. 10. Variation of the loss factor of water with increase in temperature from 0 to 100 °C.

$$\frac{E_{abs}A_{avg}}{E_{micro}} \times \frac{\lambda}{4\pi\epsilon^*_{eff}} = M_{weq} \tag{21}$$

Dielectric Correction: However, to address the dielectric property of different food i.e how easily it can absorb the microwaves, we introduce the relative dielectric property of the food with respect to water (ϵ^*_{eff}).

$$\epsilon^*_{eff} = \frac{\epsilon^{''}_{eff}}{\sqrt{(\frac{\sum_{t=0}^{\tau} r_{food}(t)}{\sigma_m})}} \tag{22}$$

where, $\sum_{t=0}^{\tau} r_{food}(t)$ is the leakage observed by RFTemp while heating the food in the microwave oven, and σ_m is the RFTemp dielectric coefficient of water of same weight as that of the food taken from the water model parameter $\sigma(m)$, introduced in the previous section.

Reflection Correction: Some food may have shallower penetration depth, compared to water, and results in larger reflection of microwaves. Larger reflection or leakage means smaller absorption, resulting in underestimation of water equivalent mass. To address this factor, we introduce reflection correction parameter (Γ^*).

$$\Gamma^* = \frac{\Gamma_{food}}{\Gamma_m} \tag{23}$$

where $\Gamma_{food} = \max(r_{food}(n) : n = [0 \cdots 15])$, n is measured in seconds and Γ_m is the reflection coefficient of the corresponding mass of water taken from the water model parameter $\Gamma(m, T)$. Thus the final water equivalent mass for the food is

$$M^*_{weq} = M_{weq} \times \Gamma^* \tag{24}$$

However, it is to be noted that, this reflection correction occurs only when $\Gamma^* > 1$. ϵ^*_{eff} and Γ^* are used to estimate the food property and are different from the parameters of water model ($\epsilon^{''}_{eff}$ and Γ).

Realization of Dielectric and Reflection Correction : Fig. 8 shows the leakage observed by water, steak, and oil, each of 200 gm when heated for 1 minute duration. If we focus on the first 15 secs time slot, we observe, the area under the curve of both steak and oil is less than water. Qualitatively it shows that these foods have a lesser affinity to absorb electromagnetic radiation than water. Thus even though smaller leakage points to higher absorption, these absorbed radiations due to lack of polar molecules in the food cannot result in dielectric heating. Fig. 8 shows that the leakage observed by steak is around 0.7 times of water while that of oil is 0.03 times of water. Dielectric correction takes care of this property of food and accurately estimates the M_{weq}. Similarly, the

reflection observed by the foods is shown in Fig. 8 by the dotted red circles. We can see steak has high reflection compared to water, which means the penetration depth is shallower. This factor is taken care of by the reflection correction parameter (Γ^*).

Dielectric value of steak measured in [35] by sophisticated cavity perturbation technique is around 58, while that of oil is around 2. Compared to the dielectric value of water (80), the dielectric property of steak relative to water is ~ 0.725 while that of oil is ~ 0.025. These values closely match with the relative leakage observed values by our system (steak - 0.7 and oil - 0.03). Fig. 9 shows the relative dielectric property of different foods with respect to water. As we can see, RFTemp relative leakage parameter closely follows the theoretical values. This verifies that the area under the leakage curve accurately estimates the dielectric property of the food. The dielectric correction parameter (ϵ^*_{eff}) introduced, thus takes care of the property of the food.

5.3.3 Temperature Estimation Block . Once the water equivalent mass is known, we can simply use the specific heat relationship to find the final temperature of the food in the microwave oven.

$$t_{final} = \frac{E_{abs}}{M^*_{weq} \times S \times \beta_{weq}} + t_{initial} \tag{25}$$

Here S is the specific heat capacity of water since the M^*_{weq} is the weight of water equivalent of the food. β_{weq} is the penetration depth correction for the water equivalent of weight M^*_{weq}. E_{abs} calculated needs to be converted to E_{heat} before using the heat capacity equation. For that reason we introduce the β_{weq} for this new M^*_{weq} which converts E_{abs} to E_{heat} before using the heat capacity equation (Eq. 25).

5.3.4 Feedback Block . This process is repeated every 15 secs. However, as we know ϵ''_{eff} of water is temperature dependent, the parameters ϵ^*_{eff}, β_m and Γ^* also varies with temperature due to the temperature dependency of the trained water model parameters. Fig. 10 shows the behaviour of ϵ''_{eff} with temperature theoretically [25]. To address this variation we use the t_{final} as a feedback into the next 15 secs slot to estimate the new ϵ''_{eff}. We introduce the feedback parameter F which is the ratio of new dielectric loss ${\epsilon''_{eff}}^T$ at temperature T to the ϵ''_{eff}.

$$F = \frac{{\epsilon''_{eff}}^T}{\epsilon''_{eff}} \tag{26}$$

$$\beta^T_m = F \times \beta_m \tag{27}$$

$${\epsilon^*_{eff}}^T = F \times \epsilon^*_{eff} \tag{28}$$

$$\Gamma^{*T} = F \times \Gamma^* \tag{29}$$

where β^T_m, ${\epsilon^*_{eff}}^T$ and Γ^{*T} are the updated values at temperature T after using feedback F.

RFTemp uses these blocks to accurately estimate the temperature of the food. The leakage observed is directly related to how the food interacts with the microwave radiation. It is to be noted that since RFTemp uses the observed leakage to determine the properties of food, the estimation of temperature is the average of the whole food rather than just the surface.

5.4 Experimental Error Correction

As we have seen in the previous section, both the dielectric correction and the reflection correction parameters depend on the leakage observed over time, $r_{food}(t)$. In this section, we address the practical experimental errors to measure the leakage and define intelligent biasing techniques to overcome it.

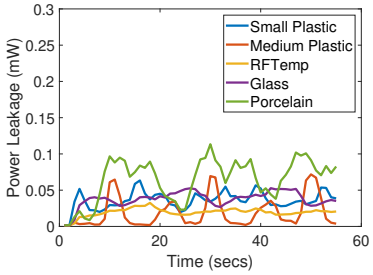

Fig. 11. Leakage observed while heating 100 gm of water across different containers. RFTemp is robust to these variations of leakage across containers.

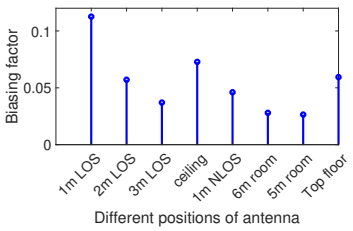

Fig. 12. Distance biasing factors at different positions in the house both line-of-sight(LOS) and non-line-of-sight (NLOS).

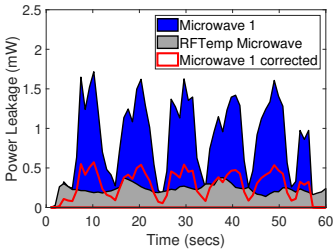

Fig. 13. Leakage observed before and after microwave correction for Microwave 1 after setting the microwave bias.

5.4.1 Container Effect. To understand the effect of containers of different shapes on the leakage observed, we microwaved 100 gm of water across different containers for 1 minute. Fig 11 shows that leakage pattern across different containers. The variations in the leakage observed are mainly due to the orientation, surface area, and material of the container. These variations affect how the food inside is exposed to radiation. However, the dielectric correction ϵ^*_{eff} and the reflection correction Γ^* being measured as a relative term to the water model, takes care of the variations of the leakage due to the container as well as the property of the food. This makes RFTemp robust to all kinds of containers of shape and material. In Fig. 11, the RFTemp is the container used for developing the water model as mentioned in Sec. 5.2. The performance of our system across different microwave containers is shown in Sec. 6.

5.4.2 Distance Effect. For different distances of the receiving antenna from the microwave oven, the leakage observed varies. It is due to the path loss of electromagnetic waves. This can affect the error in leakage estimation as the above-discussed water model does not take into consideration of the path loss. Thus to avoid this error, we introduce, distance bias (B_d).

$$B_d = \frac{E_d}{E_{RFTemp^d}} \tag{30}$$

where E_d is the leakage energy due to a different position of the rx from the microwave oven and E_{RFTemp^d} is the leakage observed at 6cm distance (used for defining water model) measured for 15 secs. We can set this biasing term while calculating the α in Eq. 19.

$$\alpha^{'} = \frac{\alpha}{B_d} \tag{31}$$

However, it is to be noted that the distance biasing is a one-time thing and can be done during the installation of RFTemp. Fig. 12 shows the biasing factor for different distances.

5.4.3 Microwave Oven Effect. Different microwave ovens have different output power (P_{micro}) and volume capacity of heating (V_{micro}). Greater is the volume, greater is the area of heating (A_{avg}). As shown in Eq.11, this affects the leakage observed outside the oven. Thus to remove this error, we define a microwave bias (B_m) solely depending on the microwave oven specifications. The amount of leakage escaping depends on the output power of the microwave oven and the volume of the microwave oven cavity.

$$B_m = \frac{E_1 \times V_1}{E_{RFTemp^m} \times V_{RFTemp^m}} \tag{32}$$

where E_1 and V_1 are the observed leakage and volume of the different microwave oven and E_{RFTemp^m} and V_{RFTemp^m} is the leakage and volume of the microwave oven used for defining water model. We can set this biasing term while calculating the α in Eq.19.

$$\alpha^{'} = \frac{\alpha}{B_m} \tag{33}$$

Like the distance biasing, this is also a one-time thing and can be performed during initialization. Fig. 13 shows the need for microwave oven biasing. The grey area shows the leakage observed by the RFTemp microwave while heating 200 gm of water, that is being used for defining the water model (1000 W 1 cu. feet). The blue area shows the leakage observed by Microwave 1 while heating 200 gm of water (1200 W and 2 cu. feet). This high leakage can result in wrong estimations. After using the microwave biasing ($B_m \sim 3$), the leakage is corrected shown by the red line.

5.4.4 Sampling Effect. If there is a mismatch in the sampling rate of the receiving data, between the trained water model and the food temperature estimation phase, the area under curve calculation will be very different. For example, if the water model is trained with a sampling rate of 5 KHz and while doing food temperature estimation the sampling rate is 20 MHz, the leakage estimation will be erroneous. This error can be corrected by a sampling bias (B_s).

$$B_s = \frac{s_{food}}{s_{wmodel}} \tag{34}$$

$$\alpha^{'} = \frac{\alpha}{B_s} \tag{35}$$

where s_{wmodel} is the sampling rate used in training for the water model and s_{food} is the sampling rate used during food temperature estimation. In Sec. 6 we have shown RFTemp's performance across different sampling rates.

Algorithm 1: RFTemp system flow

Input: Trained Water Model $(\alpha, \beta, \Gamma, \sigma)$, M_{food}, $\epsilon^{''}_{eff}$, $temp_{initial}$, $temp_{target}$, F =1
for $T \leq temp_{target}$ **do**
  for $t \leftarrow 1$ *to* τ **do**
    Record $r_{food}(t)$
  Calculate ϵ^*_{eff} and Γ^* subject to Eq.22- 23
  Recalculate using Feedback parameter (F) β^T_m, ${\epsilon^*_{eff}}^T$ and Γ^{*T} Eq. 27-29
  Estimate E_{abs} Eq.20
  Estimate M_{weq} Eq.21
  if $\Gamma^* > 1$ **then**
    $M_{weq} \leftarrow (M_{weq} \times \Gamma^*)$
  Calculate $temp_{final}$ Eq. 25
  T $\leftarrow$temp$_{final}$
  Calculate F Eq. 26

5.5 RFTemp Algorithm

Fig. 7 shows the complete workflow of RFTemp. Our system makes the following assumptions: 1) the mass of the food (M_{food}) is known; 2) initial temperature ($temp_{initial}$) is known; 3) target temperature ($temp_{target}$) is known. These are realistic assumptions as most of these information are known by the user when they use microwave oven. The input mass and initial temperature of the food need not be accurate. In Sec. 6, we have shown RFTemp

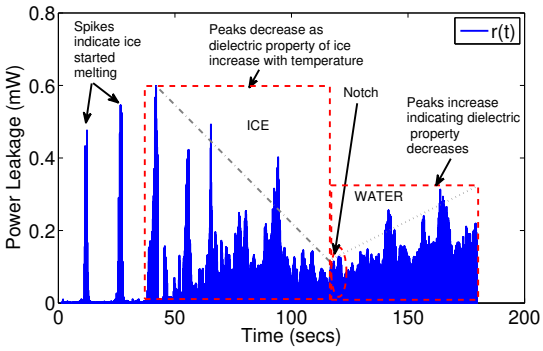

Fig. 14. Leakage pattern of ice

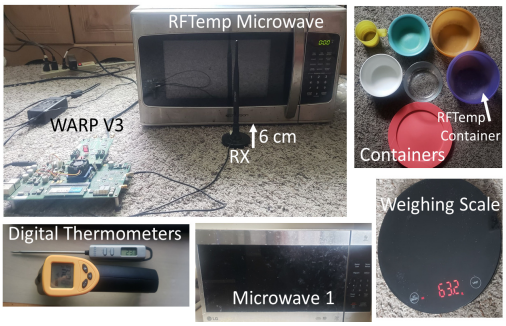

Fig. 15. Experimental setup of RFTemp

performs with high accuracy within a realistic range of input temperature and weight making our system quite flexible. The algorithm of RFTemp system flow is provide by Alg.1.

5.6 Frozen Food

Ice has a completely different dielectric property with respect to water. The water molecules in ice are packed tightly in a crystalline form. So they do not vibrate due to dielectric heating. Thus ice does not interact with electromagnetic radiation, and the loss factor (ϵ''_{eff}) of ice is very low relative to water. However, with the increase in temperature, the ϵ''_{eff} value of ice increases [22], thus it has a better absorbing capability, and leakage will decrease. This property is the opposite of water. This process will be dominant and continue till the ice melts off to water. Further heating will result in the water being warmed up. For water, ϵ''_{eff} will decrease with temperature, so the leakage peaks will increase. This phenomenon of melting ice into water will create a notch in the leakage pattern. Fig. 14 shows the leakage pattern of 150 gram of ice heated in a microwave oven for 3 minutes. As we can see, the initial spikes represent the melting phase of ice. As we know from Eq. 4 as the dielectric property increases, penetration depth increases, so the reflective power decreases. Thus with an increase in temperature, the power level of the spikes decreases. At a certain point in time, around 120 secs in Fig. 14, the leakage pattern creates a notch, and the leakage spikes increase with further increase in time following the dielectric property of water. This notch represents that the ice has melted completely. RFTemp uses this sensing technique and gets initialized after detecting the notch. The temperature of the notch is assumed to be $0^{\circ}C$. In Sec. 6 we evaluated the performance of RFTemp on various frozen food.

6 EVALUATION

To evaluate the performance of RFTemp in the real world, we build a prototype with WARP v3 software-defined radio platform [9]. The carrier frequency is set to be 2.45 GHz and the bandwidth used is 20 MHz. The power leakage is measured using omni-directional antenna [12]. We used a down-sampler to process the receiving samples at 5 kHz. Experiments are performed in a household environment. The training of water model is performed using Emerson Stainless Steel Microwave oven (1.1 cu. ft, 1000 W output power) [3]. This is referred as RFTemp Microwave. A round plastic container (2 litres in max quantity) as shown in Fig. 15 has been used as RFTemp container to train the water model [7]. LMV2031SS LG Microwave oven (2 cu. ft 1200 W)[4] has been used to verify the robustness of RFTemp across different microwaves. This is referred as Microwave 1. Etekcity

[3]Dimensions (Overall): 11.81 Inches (H) x 21.22 Inches (W) x 16.26 Inches (D)
[4]Dimensions (Overall): 16.44 Inches (H) x 29.94 Inches (W) x 15.88 Inches (D)

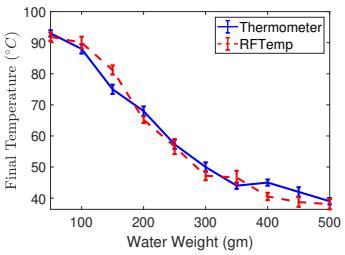

Fig. 16. RFTemp Water Model verification. RFTemp performs close to the actual thermometer measurements.

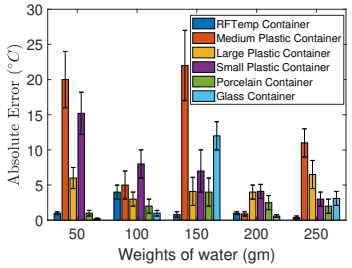

Fig. 17. Performance across different containers without setting the corrections.

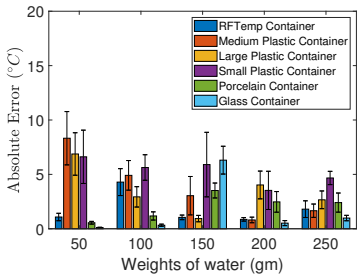

Fig. 18. Performance across different containers after setting the corrections.

Infrared (IR) Thermometer 774 and Habor 022 Digital Meat Thermometer with a probe are used to measure the temperature of different foods. We took 10 temperature measurements at different parts of the food using the probed thermometer and took the mean of them as the final measured temperature. KUBEI Digital Food Scale is used to measure the weight of different food items. Everyday household microwave containers are used to heat the food. Fig. 15 shows the setup and instruments used in this work. In all the experiments, the containers are placed at the centre of the microwave oven turntable which rotates clockwise. We evaluate the performance of RFTemp by calculating the mean absolute error between the measured temperature of the food and the RFTemp estimated temperature.

6.1 Verification of RFTemp

The training of RFTemp water model is done for weights of water ranging from 50 to 500 gm at an integral multiple of 50. For all the cases, the receiver antenna (RX) has been placed at 6 cm distance from the microwave oven front panel and the RFTemp container has been used as shown in Fig. 15. Parameters mentioned in Sec. 5.2, β, Γ, σ are calculated for the corresponding weights of water. We used a curve fitting algorithm with interpolation to make it continuous for the mentioned range of weights.

6.1.1 Water Model Accuracy . To verify the accuracy of the proposed Water Model described in Sec. 5.2, we conducted a series of experiments with the training setup shown in Fig. 15. We heated different weights of water ranging from 50-500 gm in the RFTemp container for a 1-minute duration. We set the dielectric correction and reflection correction parameters to 1 as, it is with respect to the same water model setup. We repeated the experiments 10 times and measured the final temperature with the digital thermometers. It is to be noted that, RFTemp estimates the temperature every 15 secs and the estimated value is used as an input parameter for the next slot. Fig. 16 shows the mean and standard deviations of final temperature estimated by RFTemp with the final temperature measured across the different weights. As we can see, our system estimates quite closely with the actual measurements.

6.1.2 Performance across Different Microwave Containers. We verified our system across microwave containers of different shapes and materials and repeated the same sets of experiments with water 10 times. Fig. 17 shows the mean and standard deviations of absolute error between RFTemp estimations and experimental measurements of the final temperature with the dielectric and reflection correction parameters disabled. The high error is mainly because of different orientations and surface area of the containers affect the leakage as mentioned in Sec. 5.4. However, this error can be corrected easily, by enabling the dielectric and reflection correction parameters, as shown in Fig. 18. The mean absolute error is $\sim 5^{\circ}C$. RFTemp is robust across different containers.

6.1.3 Performance across Different Distance. As we have seen in Fig. 12 the microwave oven leakage power decreases with distance and needs distance correction. This can result in erroneous estimations as the distance factor has not been included in the water model.

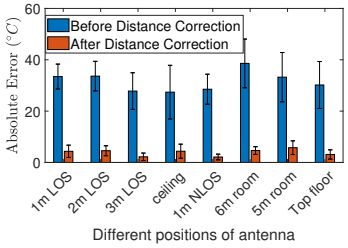

Fig. 19. Absolute error decreases less than 4°C after setting distance bias

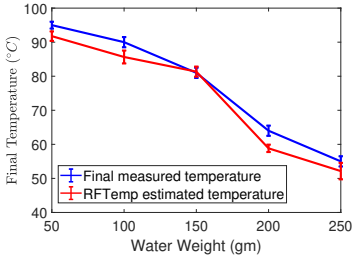

Fig. 20. RFTemp performs closely to the measured temperature estimation while using Microwave 1.

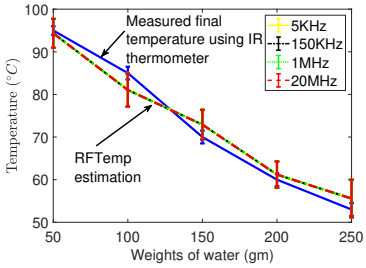

Fig. 21. Performance across different sampling rates.RFTemp performs closely to measured temperature.

We placed the receiver at 1 meter (m) line-of-sight (LOS), 2m LOS, 3m LOS, ceiling. We also experimented at non-line-of-sight (NLOS) positions like 1m NLOS, inside rooms 5m and 6m away, and even on the top floor of the house. We observed the power leakage of the microwave for 15 secs at these different positions and set the respective distance biases. We then heated 100 gm of water in the microwave oven for one minute with the receiver placed at those positions. Each experiment is repeated 10 times. Fig. 19 shows the mean and standard deviation of error in RFTemp estimation before and after setting the distance correction parameter at different positions. As we can see, RFTemp performs quite accurately with a mean error $\sim 3°C$. The error value varies from 35 to 40 $°C$ before distance correction. It is difficult to comment on if the error is directly proportional to the distance of separation. As based on the leakage, RFTemp does dielectric correction as mentioned in Sec. 5.3 that estimates the water equivalent mass. All these factors together estimate the final temperature of the food. Thus the error seems to be in the same range however factors affecting it are different.

6.1.4 Performance across Different Microwave Ovens. To verify the performance of RFTemp for different microwave ovens, we experimented on Microwave 1 previously mentioned. The power output is 1200 W and the volume capacity is 2 times than the microwave oven used for defining the water model (RFTemp microwave). We calculated the microwave bias B_m as proposed in Sec. 5.4 and experimented on different weights of water for 1 minute. Fig. 20 shows the performance of RFTemp in estimating the final temperature of the food. As we can see it closely follows the measured value with a mean error less than $\sim 3°C$.

6.1.5 Performance across Different Sampling Rates. To verify the robustness of RFTemp, we performed the water model training at 5 kHz sampling rate and tested the food temperature estimation process at different sampling rates ranging from 5 kHz to 20 MHz. In this experiment we heated 50-250 gm of water for 1 minute. As described in Sec. 5.4 we set the sampling bias each time. Fig. 21 shows the performance of RFTemp across the different sampling rates. The estimation is almost similar across different sampling rates. The mean absolute error is less than $\sim 3°C$.

6.2 Temperature Estimation Accuracy for Different Foods

In this part, we evaluate the performance of RFTemp on different food items. We used 13 different food items (5 kinds of vegetables, 5 kinds of liquids and 3 kinds of proteins) each of 100 and 200 gm of weight and heated them in the microwave oven for 1 minute. We measured the final temperature of the food using both an IR thermometer and a probed digital thermometer. Due to non-uniformity in microwave heating, different parts of

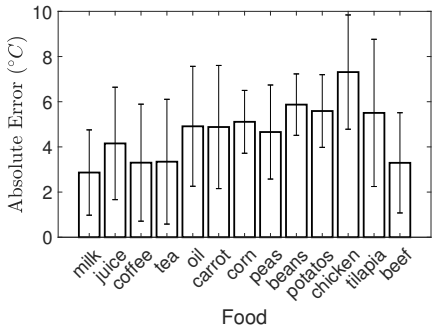

Fig. 22. Performance of RFTemp for different foods.

the food get heated differently. So, we took 10 temperature measurements at different parts of the food and took the mean of them as the final measured temperature. This process is repeated for 3 different types of containers of different size and shape. We calculated the absolute error between the temperature estimated by RFTemp and the measured final temperature to evaluate the performance of RFTemp. Since the water model has been trained for 15 secs, our system estimates the temperature of the food after every 15 secs and the estimated temperature is used as an input for the next time slot. Fig. 22 shows the performance of RFTemp across the 13 different food items. The experiments were repeated 6 times for each of the food items and the mean and standard deviation are shown. As we can see the mean absolute error for the food items is $\sim 5°C$.

6.2.1 Liquid Food vs Solid Food. Fig. 23 shows the absolute error in RFTemp estimation. We experimented on 8 different solid and 5 different liquid foods as listed on Fig. 22. The experiments have been repeated 6 times. The red circles show the absolute errors for liquid foods and the blue squares for the solid foods. Mean and standard deviations are shown for both the categories. As we can see for both solid and liquid food RFTemp estimates the final temperature with a mean absolute error $\sim 5°C$. However, our system performs better for liquid food than solid food which is mainly because of non-uniform heating of solid food.

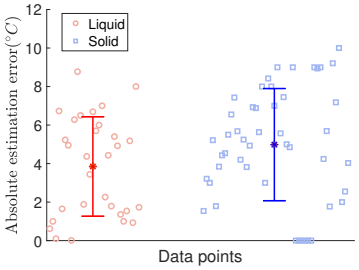

Fig. 23. Performance on liquid and solid foods

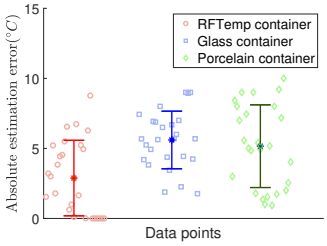

Fig. 24. Performance across different containers

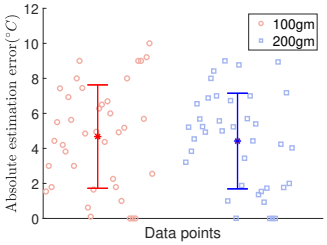

Fig. 25. Performance across different food weights

6.2.2 Across Different Containers. Fig. 24 shows the RFTemp's performance across different containers. The scatter plots show the experiments on food under each category. The experiments were repeated 26 times under each category on the food items mentioned in Fig. 22. The means and standard deviations are presented. As we can see the mean absolute error across different containers is around $5°C$ as shown by the dotted lines. However as we can see RFTemp container performs better ($\sim 3°C$ error) than the glass and porcelain containers ($\sim 5°C$

error). The increase in error is mainly because of slight variations in the dielectric and reflection correction as mentioned in Sec. 5.3. Fig. 24 shows that RFTemp is robust across different containers.

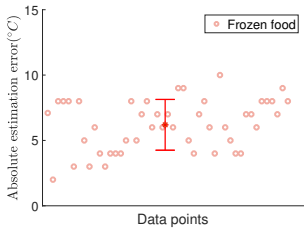

Fig. 26. Performance for different frozen foods.

6.2.3 Across Different Food Weights. To evaluate the performance of RFTemp across different weights we experimented with different food items each of 100 and 200 gm of weight. The experiments were repeated 39 times for each of 100 and 200 gm, on the food list presented earlier. Fig. 25 shows the performance of RFTemp. As we can see for both the weights RFTemp performs almost same with a mean error of $\sim 5°C$. Thus variation of weights does not affect the performance of our system.

6.2.4 Frozen Food. As we have discussed in Sec. 5.6, to estimate the temperature of frozen food, RFTemp is initialized by estimating the notch in the time varied power leakage pattern. To experiment system performance, we heated 7 different ready-to-eat frozen food in microwave oven and estimated the temperature at the end of 3 minutes. We repeated the experiments 5 times on each of them. Fig. 26 shows the performance of RFTemp. As we can see, it can estimate the temperature with a mean error $\sim 7°C$. Error increases due to error in the notch detection. RFTemp can easily differentiate normal foods from the frozen foods by the initial input temperature.

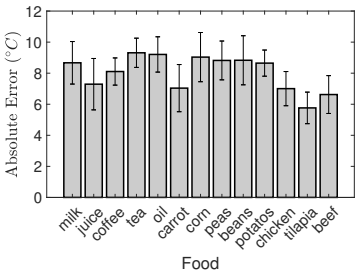

Fig. 27. Performance for 15 secs decision boundary

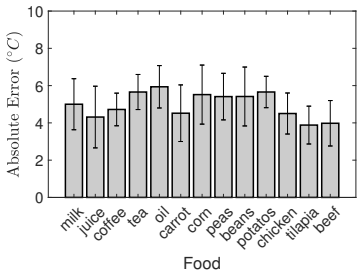

Fig. 28. Performance for 7.5 secs decision boundary

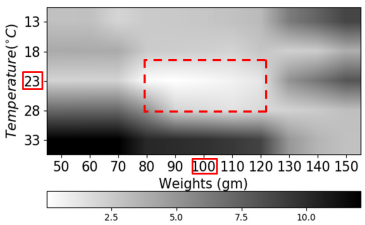

Fig. 29. Admissible range for food weight and initial temperature

6.2.5 Verification of RFTemp Algorithm. To verify the performance of RFTemp algorithm, we conducted experiments on the 13 different food items as listed in Fig. 22 for 1 minute. We set a random target temperature each time and measured the absolute error between the target temperature and the temperature when RFTemp notifies to stop the microwave oven. The experiments were repeated 6 times on each of the food items. The decision boundary was fixed at 15 secs, that is RFTemp will notify only after every 15 secs of interval. Fig. 27 shows the absolute error with 15 secs decision boundary. The mean error is $\sim 8°C$, which is mainly because of the time slot of the decision boundary. It is to be noted that RFTemp still estimates the actual temperature quite accurately in real time. However, due to the time slot of 15 secs, the food can get overheated compared to the target temperature. This is more prominent on food with smaller weights as they get heated faster and there is a considerable temperature difference in consecutive slots. However, using a decision boundary of 7.5 secs, the

error is reduced to $\sim 5°C$ as shown in Fig. 28. This can be achieved easily by training the water model for 7.5 secs. Further reduction of decision boundary is unrealistic as the water model will not be accurate as the increase in temperature for different weights of water during the training phase will be nominal. It is to be noted that accumulation error takes place in every time slot, however, this error is very nominal and does not affect the performance of RFTemp as shown in the Fig. 28.

RFTemp assumes the mass of the food and the initial temperature of the food are known by the user before using the microwave oven. However, these are not hard assumptions. Fig. 29 shows the error in temperature estimation for 100 gm of water with an initial temperature of $23°C$. The actual values are marked with red boxes. The dotted red box shows the admissible errors for the range of weight and temperature values centered around the actual measured input values. As we can see for weights from 80-120 (± 20 gm) and temperature 18-28 (± $5°C$), the estimated errors are below $5°C$. This is valid for food with any weight. Thus even if users have a rough idea about the food weight and temperature, RFTemp can perform with high accuracy.

6.2.6 Across Complex Food. To evaluate the performance of RFTemp on different food items, we conducted experiments in a household environment for a duration of 30 days. We experimented on 35 different everyday food items of different weights and initial temperature. To be noted, these food items were heated in random microwave containers for an average duration of 1-3 minutes. We measured the final temperature using a probed food thermometer as a baseline. We measured at different thickness of the food and estimated the average of the measurements as the final temperature. To evaluate the performance of infrared sensors and thermometers, we measured the temperature of the food using a contactless IR thermometer.

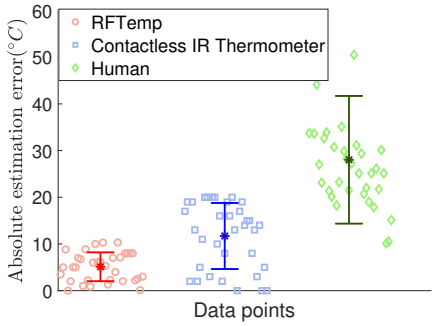

Fig. 30. RFTemp performance on complex food

We also let the users estimate the final temperature based on their experience of microwave oven heating mechanism. The green points in Fig. 30 shows the human error for all the food items. As we can see, the mean human error in estimation is above $\sim 25°C$. This proves that it is not trivial for a human being to estimate the temperature of the food which results in either overheating or reheating again. The blue scatter plots show the error of IR thermometer. The mean error in this case is $\sim 13°C$. This error is mainly because IR thermometers can only pick the surface temperature rather than the actual average temperature of the food. On the other hand, the red scatter plots show the performance of RFTemp on these different foods. As we can see, RFTemp has the least mean absolute error of $\sim 5°C$ among the others. Even though both RFTemp's and IR thermometer's performance is very close to one another, RFTemp performs better on solid food compared to IR thermometer. Thus RFTemp, as proposed, can estimate the temperature of the food inside the microwave oven with very high accuracy, 2x better than IR thermometers.

7 DISCUSSION

7.1 RFTemp Water Model Granularity

7.1.1 Training Period. RFTemp water model is trained for 15 secs of duration. That is our system senses leakage every 15 secs interval and estimates the temperature of the food. The 15 secs interval has been chosen because it takes around the same time for the turntable in most microwave ovens to complete one cycle of rotation. It is to be noted that in every 15 seconds interval, RFTemp uses a feedback technique to estimate the relative parameters for the next interval. Thus estimation errors in each section can add up in every interval. However, in Sec. 6 we showed that RFTemp can estimate the temperature with a mean error of $\sim 5°C$ even heating food for 3 minutes. Thus the addition of error is very nominal. This error can further decrease if the duration of the water model training increases as RFTemp will observe more samples to train the water model. However, there will be a trade-off as with the increase in duration, RFTemp can estimate temperature every such interval. For example, if the water model is trained for 60 secs, RFTemp will estimate temperature every 60 secs resulting in overheating as shown in Fig. 27.

7.1.2 Training Weights. The water model in RFTemp is trained for food having weights of integral multiple of 50 gm between 50 to 500 gm and a curve fitting is used to estimate the parameters for intermediate weights. The training set can be improved by experimenting on weights of water with a smaller interval. The weight range is very realistic as most of the everyday food that is being heated in a microwave oven falls within that range. However, RFTemp can easily incorporate more weights by extending the training phase for higher amounts of water.

7.2 RFTemp Thawing and Cooking

Microwave ovens are used mostly for reheating purposes. Surveys [1, 51] show that majority of the people are using microwave ovens for heating purposes for 1-3 minutes on average. However, in some cases, microwave ovens are used for thawing and cooking food. Our system does not handle the thawing and cooking of food cases directly. Thawing is the process of ice or any frozen substance becoming liquid by getting heated [2]. RFTemp can be used for thawing purposes using the notch detection technique introduced by frozen food in Sec. 5.6. However, cooking is a more complex process that involves the change of state of water, like cooking pasta and rice in boiling water. RFTemp water model does not cover the change of state of water which involves latent heat of evaporation. Also the volume of the food changes during cooking which makes the system very complex for RFTemp to estimate. However, RFTemp can train the water model with some intelligent cooking techniques to incorporate the latent heat of evaporation of water. This has been left for future research.

7.3 RFTemp Error Accumulation

For scenarios using sampling, distance and microwave biasing parameters, error accumulation in the final estimation can take place. However, such errors will be very nominal and can result in mean 1-2$°C$ extra error.

7.4 RFTemp Deployment

The question is how RFTemp can be integrated into existing systems. As we have mentioned in Sec. 4, microwave operates in the same frequency range as other wireless applications like WiFi. Thus the leakage from the microwave oven interferes with the WiFi communication systems. Commercial Access Point (AP) can observe the wireless activity of its channel like in [39, 40] and measure the leakage due to microwave oven both in presence and absence of WiFi packet transfer and reception. Most of these commercial access points have software platforms that can be used for user-defined applications and can also forward data to the cloud or remote servers without any functional degradation [24, 39]. Thus RFTemp can be easily deployed in the commercial access

points using these features. During the setup phase, the initial parameters of RFTemp water model can be fed into a remote server connected with the APs. Then the empty microwave oven in the household is run for 15 secs. RFTemp running in APs can be self initialized when it detects high leakage and measures the time varied leakage and send it to the server. This is used to set up the biasing parameters as mentioned in Sec. 5.4. This is a one-time thing that is done during the setup phase. Once the setup phase is over, RFTemp can be used for temperature estimation. During heating of food, the user provides the weight of the food, initial temperature, and target temperature values to a cloud application and starts the microwave oven. APs can detect microwave leakage and forward it to the cloud server. Using the RFTemp algorithm proposed in Sec. 5.5, the cloud application estimates the temperature of the food inside the microwave oven. Once it has reached the target temperature, it can notify the user to stop further heating. It is to be noted that RFTemp deployment does not require any update on WiFi protocol and can be easily implemented in commercial APs. It also does not require any changes on the commercial microwave ovens. Thus it can be easily integrated into the existing systems.

8 CONCLUSION

In this paper, we present RFTemp, the first practical RF sensing technique to measure the temperature of the food inside the microwave oven. Our evaluations show that, RFTemp is robust to all varieties of food types, microwave ovens, microwave containers and can be easily integrated into the commercial systems. Thus, RFTemp converts commercial microwave oven into a smart microwave oven without any hardware change, which can estimate the food temperature and notify the users when the target temperature has reached, with great accuracy.

ACKNOWLEDGMENTS

We thank the anonymous reviewers and the CoSyNe Communication Systems and Networking group for their feedback on the paper. We thank the National Science Foundation (NSF) for supporting this effort through the projects; NSF 2128567, NSF 2007581 and NSF 2018912.

REFERENCES

[1] 2009. *Americans are eating at home more; microwave usage increases but not cooking.* https://www.npd.com/wps/portal/npd/us/news/press-releases/pr_091112/.
[2] 2013. *The Big Thaw — Safe Defrosting Methods.* https://www.fsis.usda.gov/food-safety/safe-food-handling-and-preparation/food-safety-basics/big-thaw-safe-defrosting-methods.
[3] 2016. *Penetration Depth.* https://genuineideas.com/ArticlesIndex/wave.html.
[4] 2017. *Microwave Oven Radiation.* https://www.fda.gov/radiation-emitting-products/resources-you-radiation-emitting-products/microwave-oven-radiation#Microwave_Oven_Safety_Standard.
[5] 2018. *FLiR Dev Kit.* https://www.sparkfun.com/products/13233/.
[6] 2019. *June Intelligent Oven.* https://juneoven.com.
[7] 2020. *CrystalWave® PLUS 2-qt./2 L Round.* https://www.tupperware.com/crystalwave-plus-2-qt-2-l-round-catalog-summer-2020/.
[8] 2020. *Total unit shipments of microwave ovens in the U.S. from 2005 to 2019 (in millions).* https://www.statista.com/statistics/220122/unit-shipments-of-microwave-ovens/.
[9] 2020. *WARP Project.* http://warpproject.org.
[10] 2021. *Cavity magnetron.* https://en.wikipedia.org/wiki/Cavity_magnetron.
[11] 2021. *Dielectric heating.* https://en.wikipedia.org/wiki/Dielectric_heating.
[12] 2021. *VERT2450 Antenna.* https://www.ettus.com/all-products/vert2450/.
[13] M. Al-Kuwari, A. Ramadan, Y. Ismael, L. Al-Sughair, A. Gastli, and M. Benammar. 2018. Smart-home automation using IoT-based sensing and monitoring platform. In *2018 IEEE 12th International Conference on Compatibility, Power Electronics and Power Engineering (CPE-POWERENG 2018).* 1–6. https://doi.org/10.1109/CPE.2018.8372548
[14] Edward Belotserkovsky, Ofer Shenfeld, and Abraham Katzir. 1994. Infrared fiberoptic temperature control of the heating process in a microwave oven. *IEEE transactions on microwave theory and techniques* 42, 5 (1994), 901–903.
[15] John Bows and Ketan Joshi. 1992. Infrared imaging feels the heat in microwave ovens. *Physics World* 5, 8 (1992), 21.

[16] Gabe Cohn, Sidhant Gupta, Jon Froehlich, Eric Larson, and Shwetak N Patel. 2010. GasSense: Appliance-level, single-point sensing of gas activity in the home. In *International Conference on Pervasive Computing*. Springer, 265–282.
[17] G Cuccurullo, L Giordano, D Albanese, Luciano Cinquanta, and M Di Matteo. 2012. Infrared thermography assisted control for apples microwave drying. *Journal of food engineering* 112, 4 (2012), 319–325.
[18] Ashim K Datta. 2001. *Handbook of microwave technology for food application*. CRC Press.
[19] Abe Davis, Katherine L Bouman, Justin G Chen, Michael Rubinstein, Fredo Durand, and William T Freeman. 2015. Visual vibrometry: Estimating material properties from small motion in video. In *Proceedings of the ieee conference on computer vision and pattern recognition*. 5335–5343.
[20] Abe Davis, Michael Rubinstein, Neal Wadhwa, Gautham J Mysore, Fredo Durand, and William T Freeman. 2014. The visual microphone: Passive recovery of sound from video. (2014).
[21] Jon E Froehlich, Eric Larson, Tim Campbell, Conor Haggerty, James Fogarty, and Shwetak N Patel. 2009. HydroSense: infrastructure-mediated single-point sensing of whole-home water activity. In *Proceedings of the 11th international conference on Ubiquitous computing*. 235–244.
[22] Shuji Fujita, Takeshi Matsuoka, Toshihiro Ishida, Kenichi Matsuoka, and Shinji Mae. 2000. A summary of the complex dielectric permittivity of ice in the megahertz range and its applications for radar sounding of polar ice sheets. In *Physics of ice core records*. Hokkaido University Press, 185–212.
[23] Sidhant Gupta, Matthew S Reynolds, and Shwetak N Patel. 2010. ElectriSense: single-point sensing using EMI for electrical event detection and classification in the home. In *Proceedings of the 12th ACM international conference on Ubiquitous computing*. 139–148.
[24] Milad Heydariaan and Omprakash Gnawali. 2016. WiFi access point as a sensing platform. In *2016 IEEE Global Communications Conference (GLOBECOM)*. IEEE, 1–6.
[25] Udo Kaatze. 1989. Complex permittivity of water as a function of frequency and temperature. *Journal of Chemical and Engineering Data* 34, 4 (1989), 371–374.
[26] Tareq Khan. 2018. Smart Microwave Oven with Image Classification and Temperature Recommendation Algorithm. *International Journal of Electrical & Computer Engineering (2088-8708)* 8, 6 (2018).
[27] Tareq Khan. 2018. Towards an autonomous temperature feedback microwave oven with thermal imaging. In *2018 IEEE International Conference on Electro/Information Technology (EIT)*. IEEE, 0444–0448.
[28] Tareq Khan. 2020. An intelligent microwave oven with thermal imaging and temperature recommendation using deep learning. *Applied System Innovation* 3, 1 (2020), 13.
[29] Christine Kühnel, Tilo Westermann, Fabian Hemmert, Sven Kratz, Alexander Müller, and Sebastian Möller. 2011. I'm home: Defining and evaluating a gesture set for smart-home control. *International Journal of Human-Computer Studies* 69, 11 (2011), 693–704.
[30] Zhenfeng Li, GSV Raghavan, and Valérie Orsat. 2010. Optimal power control strategies in microwave drying. *Journal of Food Engineering* 99, 3 (2010), 263–268.
[31] Cui Liyan, Gao Min, Xiong Qingyu, Wen Junhao, and Xie Ning. 2015. Temperature monitoring based on image processing for intelligent microwave heating. In *The 27th Chinese Control and Decision Conference (2015 CCDC)*. IEEE, 1397–1401.
[32] James Clerk Maxwell. 1873. *A treatise on electricity and magnetism*. Vol. 1. Oxford: Clarendon Press.
[33] Juan Monzó-Cabrera, Juan Luis Pedreño-Molina, and A Toledo. 2009. Feedback control procedure for energy efficiency optimization of microwave-heating ovens. *Measurement* 42, 8 (2009), 1257–1262.
[34] Ghulam Muhammad, SK Md Mizanur Rahman, Abdulhameed Alelaiwi, and Atif Alamri. 2017. Smart health solution integrating IoT and cloud: A case study of voice pathology monitoring. *IEEE Communications Magazine* 55, 1 (2017), 69–73.
[35] T OhIsson, NE Bengtsson, and PO Risman. 1974. The frequency and temperature dependence of dielectric food data as determined by a cavity perturbation technique. *Journal of microwave power* 9, 2 (1974), 129–145.
[36] OpenStax. 2020. Energy Carried by Electromagnetic Waves. https://chem.libretexts.org/@go/page/4451 [Online; accessed 2021-04-04].
[37] Shijia Pan, Mario Berges, Juleen Rodakowski, Pei Zhang, and Hae Young Noh. 2019. Fine-grained recognition of activities of daily living through structural vibration and electrical sensing. In *Proceedings of the 6th ACM International Conference on Systems for Energy-Efficient Buildings, Cities, and Transportation*. 149–158.
[38] Shwetak N Patel, Thomas Robertson, Julie A Kientz, Matthew S Reynolds, and Gregory D Abowd. 2007. At the flick of a switch: Detecting and classifying unique electrical events on the residential power line (nominated for the best paper award). In *International Conference on Ubiquitous Computing*. Springer, 271–288.
[39] Ashish Patro and Suman Banerjee. 2014. COAP: A software-defined approach for home WLAN management through an open API. In *Proceedings of the 9th ACM workshop on mobility in the evolving internet architecture*. 31–36.
[40] Ashish Patro, Srinivas Govindan, and Suman Banerjee. 2013. Observing home wireless experience through wifi aps. In *Proceedings of the 19th annual international conference on Mobile computing & networking*. 339–350.
[41] RW Powitz. 2006. best of the best: A critical look at basic inspection tools. *Foodsafety magazine* (2006).
[42] Qifan Pu, Sidhant Gupta, Shyamnath Gollakota, and Shwetak Patel. 2013. Whole-home gesture recognition using wireless signals. In *Proceedings of the 19th annual international conference on Mobile computing & networking*. 27–38.

[43] Indra Riyanto, Lestari Margatama, Hakim Hakim, Dicky Edwin Hindarto, et al. 2018. Motion sensor application on building lighting installation for energy saving and carbon reduction joint crediting mechanism. *Applied System Innovation* 1, 3 (2018), 23.

[44] Isidro Sanchez, Julio R Banga, and Antonio A Alonso. 2000. Temperature control in microwave combination ovens. *Journal of Food Engineering* 46, 1 (2000), 21–29.

[45] Mei H Sun, Kenneth A Wickersheim, and James Kim. 1989. Fiberoptic temperature sensors in the medical setting. In *Optical Fibers in Medicine IV*, Vol. 1067. International Society for Optics and Photonics, 15–21.

[46] Wei Sun, Tuochao Chen, Jiayi Zheng, Zhenyu Lei, Lucy Wang, Benjamin Steeper, Peng He, Matthew Dressa, Feng Tian, and Cheng Zhang. 2020. VibroSense: Recognizing Home Activities by Deep Learning Subtle Vibrations on an Interior Surface of a House from a Single Point Using Laser Doppler Vibrometry. *Proceedings of the ACM on Interactive, Mobile, Wearable and Ubiquitous Technologies* 4, 3 (2020), 1–28.

[47] Michael Vollmer. 2004. Physics of the microwave oven. *Physics Education* 39, 1 (2004), 74.

[48] Qian Wan, Yiran Li, Changzhi Li, and Ranadip Pal. 2014. Gesture recognition for smart home applications using portable radar sensors. In *2014 36th annual international conference of the IEEE engineering in medicine and biology society*. IEEE, 6414–6417.

[49] Xuyu Wang, Lingjun Gao, Shiwen Mao, and Santosh Pandey. 2016. CSI-based fingerprinting for indoor localization: A deep learning approach. *IEEE Transactions on Vehicular Technology* 66, 1 (2016), 763–776.

[50] Wei Wei, Akihiro Nakamata, Yoshihiro Kawahara, and Tohru Asami. 2015. Food Recognition via Monitoring Power Leakage from a Microwave Oven. *Journal of Information Processing* 23, 6 (2015), 835–844.

[51] Alison Williams. 2012. Surveys of microwave ovens in US homes. (2012).

[52] Yang Zhang, Gierad Laput, and Chris Harrison. 2018. Vibrosight: Long-range vibrometry for smart environment sensing. In *Proceedings of the 31st Annual ACM Symposium on User Interface Software and Technology*. 225–236.